UNCLASSIFIED
SECURITY CLASSIFICATION OF THIS PAGE (When Data Entered)

ARO 15878.3-P

AD A109142

DTIC FILE COPY

REPORT DOCUMENTATION PAGE

READ INSTRUCTIONS BEFORE COMPLETING FORM

1. REPORT NUMBER: P-15878-P	2. GOVT ACCESSION NO.: AD-A109 142
3. RECIPIENT'S CATALOG NUMBER:	
4. TITLE (and Subtitle): The Electronic and Atomic Structure of Diamond Surface and Effects of Hydrogen Termination	5. TYPE OF REPORT & PERIOD COVERED: Final Report 7/1/78 - 6/30/81
	6. PERFORMING ORG. REPORT NUMBER:
7. AUTHOR(s): B. B. Pate, P. J. Jupiter, I. Lindau, and W. E. Spicer	8. CONTRACT OR GRANT NUMBER(s): DAAG-78-G-0130
9. PERFORMING ORGANIZATION NAME AND ADDRESS: Stanford University, Stanford, Calif. 94305 (12)	10. PROGRAM ELEMENT, PROJECT, TASK AREA & WORK UNIT NUMBERS: (29)
11. CONTROLLING OFFICE NAME AND ADDRESS: U. S. Army Research Office, Post Office Box 12211, Research Triangle Park, NC 27709	12. REPORT DATE: November 2, 1981
	13. NUMBER OF PAGES: 6, plus two appendixes
14. MONITORING AGENCY NAME & ADDRESS (if different from Controlling Office)	15. SECURITY CLASS. (of this report): Unclassified
	15a. DECLASSIFICATION/DOWNGRADING SCHEDULE:

LEVEL II

16. DISTRIBUTION STATEMENT (of this Report)

Approved for public release; distribution unlimited.

DTIC ELECTE JAN 4 1982 S D H

17. DISTRIBUTION STATEMENT (of the abstract entered in Block 20, if different from Report)

NA

18. SUPPLEMENTARY NOTES

The view, opinions, and/or findings contained in this report are those of the author(s) and should not be construed as an official Department of the Army position, policy, or decision, unless so designated by other documentation.

19. KEY WORDS (Continue on reverse side if necessary and identify by block number)

Diamond, hydrogen, photoemission spectroscopy, photon stimulated desorption, phonons, surface reconstruction, semiconductor.

20. ABSTRACT (Continue on reverse side if necessary and identify by block number)

The electronic and atomic structure of the diamond (111) surface and the effects of hydrogen termination are studied using photoemission, photon stimulated desorption, low energy electron diffraction, and Auger electron spectroscopy. Hydrogen termination results in a 1 x 1 surface with no filled surface states in or near the band gap region. A high temperature anneal (~1000°C) removes the hydrogen and results in a 2 x 2/2 x 1 surface structure.

DD FORM 1 JAN 73 1473 EDITION OF 1 NOV 65 IS OBSOLETE

332 350

UNCLASSIFIED
SECURITY CLASSIFICATION OF THIS PAGE (When Data Entered)

FINAL REPORT

ARO PROJECT NUMBER: P15878-P

PERIOD COVERED BY REPORT: July 1, 1978 through June 30, 1981

TITLE: The Electronic and Atomic Structure of Diamond Surface and Effects of Hydrogen Termination

CONTRACT NUMBER: DAAG-78-G-0130

NAME OF INSTITUTION: Stanford University

AUTHORS OF REPORT: B. B. Pate, P. J. Jupiter, I. Lindau, and W. E. Spicer

DATE: December 2, 1981

LIST OF MANUSCRIPTS:

Electronic Structure of the Diamond (111) 1 x 1 surface: Valence-band Structure, band bending, and bandgap states, B. B. Pate, T. Ohta, I. Lindau and W. E. Spicer, J. Vac. Sci. Technol. 17, 1087 (1980).

Formation of Surface States on the (111) Surface of Diamond, B. B. Pate, P. M. Stefan, C. Binns, P. J. Jupiter, M. L. Shek, I. Lindau and W. E. Spicer, J. Vac. Sci. Technol. 19, 349 (1981).

SCIENTIFIC PERSONNEL Supported by this project and degrees awarded during this reporting period:

W. E. Spicer, PI; I. Lindau, PI; J. N. Miller, Research Associate, B. B. Pate, graduate student; P. J. Jupiter, graduate student.

THE ELECTRONIC AND ATOMIC STRUCTURE OF DIAMOND SURFACE AND EFFECTS OF HYDROGEN TERMINATION

A program which investigated aspects of the atomic and electronic structure of diamond was begun at Stanford in June, 1978. This report summarizes the advances made in the understanding of bulk diamond and of the diamond (111) surface over the three years which followed. To date, our results have been presented at two conferences (The Seventh Annual Physics of Compound Semiconductors [PCSI-7] Conference in January 1980, and at the PCSI-8 in January, 1981). Two publications have resulted from our study. Our work prior to February, 1981 is thoroughly discussed in these publications, and therefore they are included as Appendix I and Appendix II to this final report. We will discuss here only those results (the majority of which were obtained in the last three months of the contract period) which have yet to be submitted for publication. As proposed in our renewal proposal of this ARO contract, we hope to complete our study of diamond under ARO sponsorship.

Early in our work with diamond, we expected that hydrogen may be terminating the surface (see Appendix I and II). We suspected that termination of the surface with hydrogen removed surface states from the bandgap region and altered the surface reconstruction which otherwise would have occurred. Since the study of Schottky barriers on diamond is an eventual aim of our work, both the knowledge of the presence of hydrogen and the understanding of the effects of hydrogen termination is extremely important. Our most recent results confirm hydrogenation of the (111) 1 x 1 surface and give additional insight concerning electronic effects of hydrogen termination. These results are discusssed in Section A below.

As reported previously in our progress reports, temperature sensitive oscillations in the near bandgap photo-electric yield have been observed in

diamond. These phonon-related structures can be observed directly by photoemission due to a combination of the large optical phonon energies of diamond (~ 170 meV) and the observed effective negative electron affinity of diamond (111) 1 x 1 (see Appendix I). We report our most recent results in Section B.

A. Effects and Consequences of Hydrogen Termination

We have studied the diamond (111) surface using photoemission spectroscopy (PES) and a variety of photoyield spectroscopies, including studies at and near the carbon 1s ionization threshold ($h\nu \approx 285$ eV). Using the technique of photon stimulated ion desorption (PSID), we find that, upon ionization of the C 1s core level, hydrogen ions desorb from the (111) 1 x 1 surface via the Knotek-Feibelman Auger decay mechanism. The striking similarity in structure of the KLL Auger electron yield to the hydrogen ion yield (see Figure 1) confirms that the desorption results from the severance of the diamond-hydrogen bond. The diamond (111) 1 x 1 surface has previously been found to reconstruct upon annealing (~ 950°C) to form a 2 x 2/2 x 1 surface with a band of surface states near the valence band maximum (see Appendix II). Our PSID experiments find no hydrogen desorption from the reconstructed surface, indicating that the anneal has served the purpose of driving the hydrogen from the surface. In separate experiments, we find (using PES) that, while annealing to 950°C results in the growth of the surface state emission near the valence band maximum (a 2 x 2/2 x 1 surface), exposure to activated hydrogen removes those electronic states.

The empty local density of states at the diamond surface can be explored with PSID. Carbon K-edge PSID of hydrogen is a selective probe, which samples only those carbon atoms which have hydrogen attached. We find, by comparison with bulk sensitive X-ray fluorescence yield (labeled total photoyield in Figure 2), that at the surface there is an enhanced p-like local density of

states near the conduction band minimum for the hydrogen terminated surface carbon atoms. This data is shown in Figure 2.

B. Phonon Effects in Transmission and Photo-electric Yield

Further experiments have been done to explain the previously reported structure found in the photoelectric yield of diamond between 5.5 and 6.5 eV. The photoelectric yield experiment was repeated on a freshly polished (111) surface at room temperature and 120°K (See Figure 3). At the lower temperature the structure sharpened and was shifted to higher energy by 0.03 eV. In addition a transmission measurement was made on a (110) surface of a 12 micron thick diamond. The transmission data was taken at room temperature and 130°K. Except for a rinse in alcohol there was no surface preparation. Three absorption peaks were noted between 5.5 and 5.1 eV with spacings of approximately 170 meV which corresponds to the spacing of the structure found in the photoelectric yield. Also a shift to higher energy of approximately 0.02 eV was noted at the lower temperature. Further analysis of the data will continue and be reported in progress reports for the proposed renewal contract.

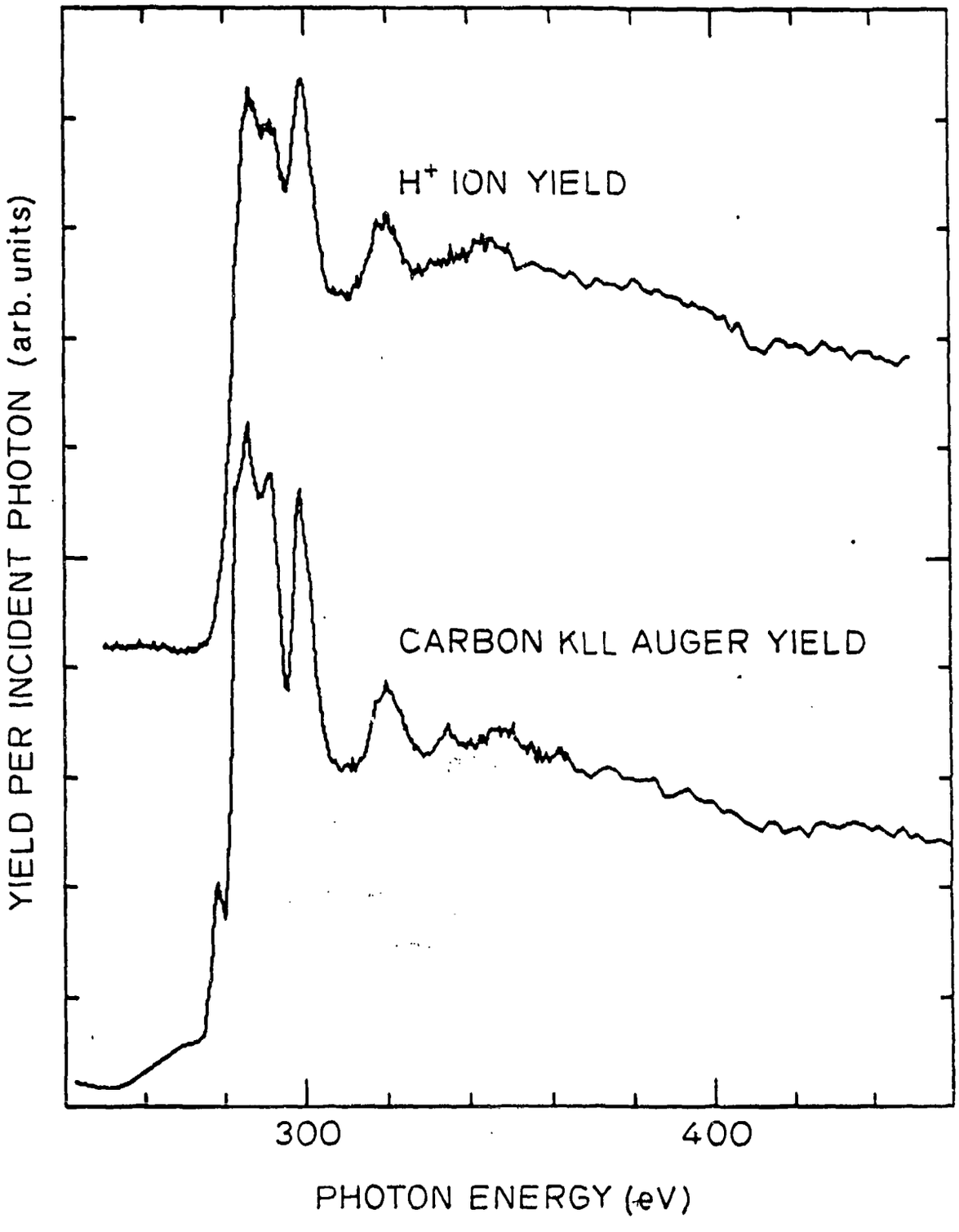
H+ ION YIELD
CARBON KLL AUGER YIELD
YIELD PER INCIDENT PHOTON (arb. units)
300
400
PHOTON ENERGY (eV)

FIGURE 1

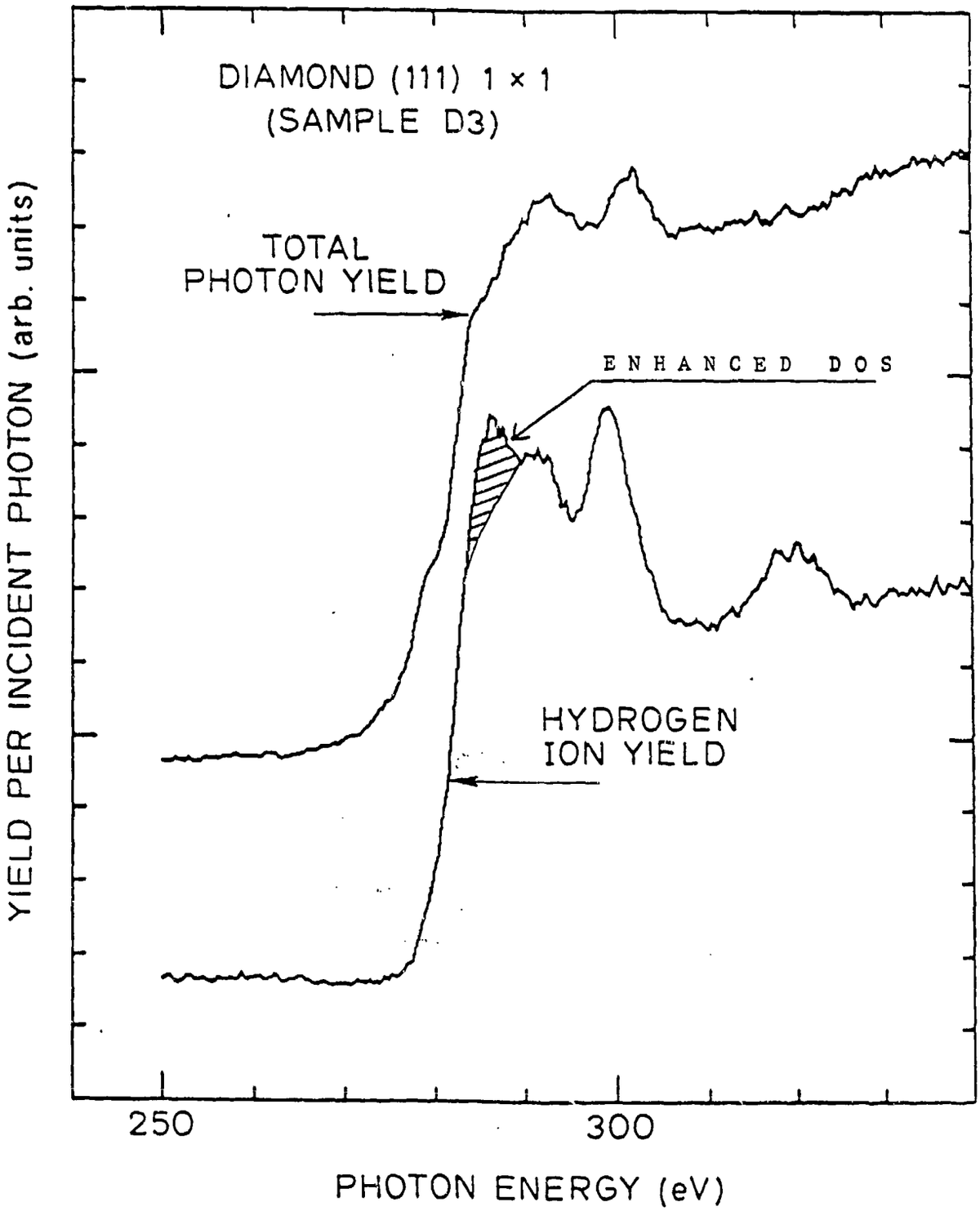
DIAMOND (111) 1 × 1
(SAMPLE D3)
TOTAL
PHOTON YIELD
ENHANCED DOS
HYDROGEN
ION YIELD
YIELD PER INCIDENT PHOTON (arb. units)
250
300
PHOTON ENERGY (eV)

FIGURE 2

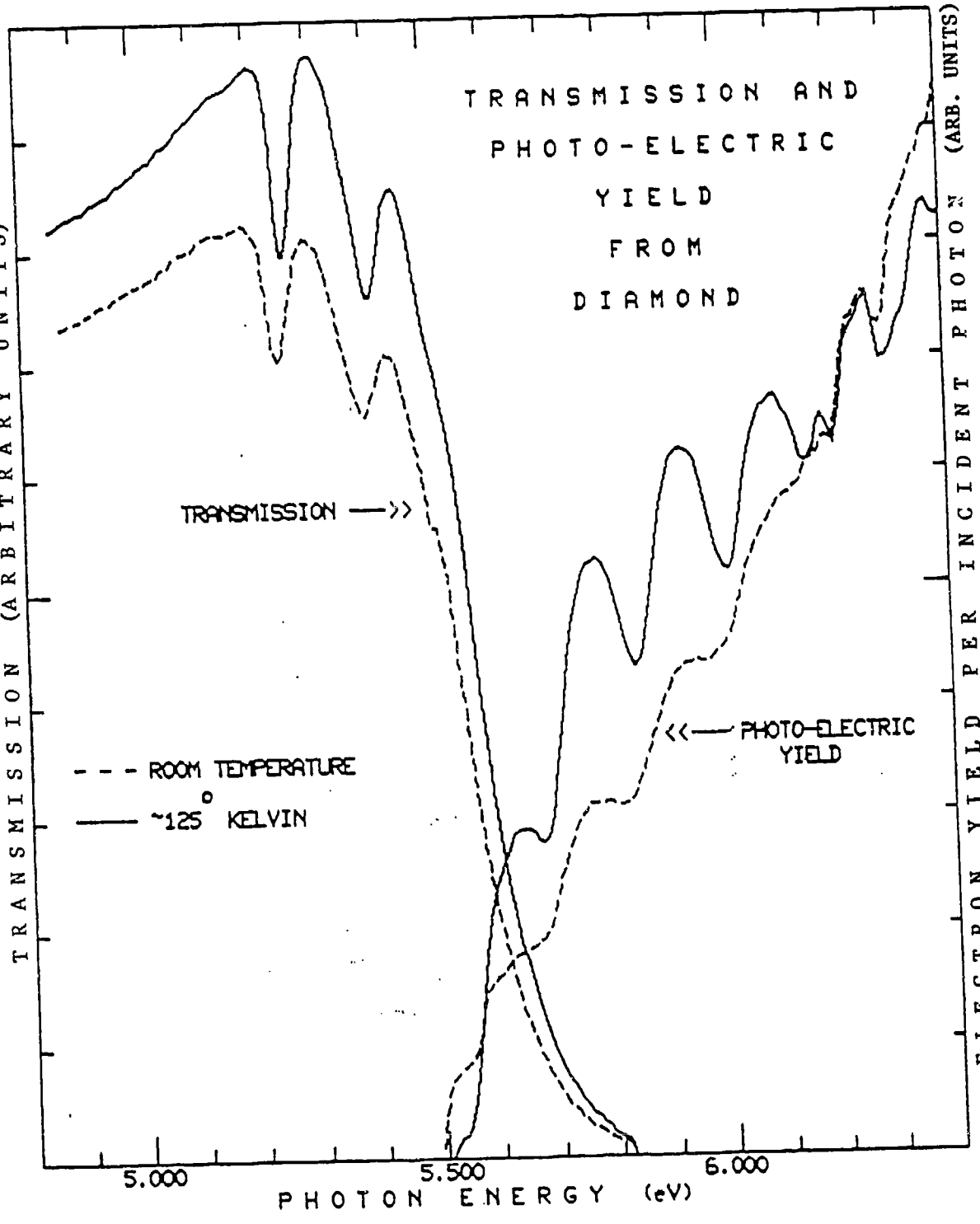
TRANSMISSION AND
PHOTO-ELECTRIC
YIELD
FROM
DIAMOND
TRANSMISSION (ARBITRARY UNITS)
ELECTRON YIELD PER INCIDENT PHOTON (ARB. UNITS)
TRANSMISSION ——>>
<<—— PHOTO-ELECTRIC YIELD
- - - ROOM TEMPERATURE
—— ~125° KELVIN
5.000
5.500
6.000
PHOTON ENERGY (eV)

FIGURE 3

Electronic structure of the diamond (111) 1×1 surface: Valence-band structure, band bending, and band gap states

B. B. Pate and W. E. Spicer[a)]

Stanford Electronics Laboratories, Stanford University, Stanford, California 94305

T. Ohta[b)] and I. Lindau

Stanford Synchroton Radiation Labortory, Stanford University, Stanford, California 94305

(Received 28 March 1980; accepted 21 May, 1980)

Photoemission, LEED, and AES measurements were made on the mechanically polished (111) surface of a type IIa diamond. No emission from filled states in the fundamental gap was found over the photon energy range 13.3 eV $\lesssim \hbar\omega \lesssim$ 200 eV. This result, coupled with the sharp 1×1 LEED patterns which were obtained and the relative cleanliness (of elements which can be detected by AES) of the diamond ($\lesssim$1 at.% oxygen, <0.5 at.% Si) suggests hydrogen termination of the lattice. Photoelectric yield measurements demonstrate the photoelectric threshold to be at band gap energy radiation. Investigation of the photoemission electron distribution curves (EDC's) shows that, while the electron affinity at the surface is always positive, band bending is sufficient to result in an effective negative electron affinity under certain conditions. A variable surface dipole on the atomic scale, possibly due to the adsorption–desorption of a background gas, is reported. A study of the relative cross section of the upper (p-like) versus the lower (s-like) portion of the diamond valence band indicates comparable cross sections at a photon energy $\hbar\omega = 160$ eV.

PACS numbers: 79.60.Eq, 73.30. + y, 73.20. − r, 71.20. + c

I. INTRODUCTION

Diamond holds a unique position among column IV elemental solids. Of interest is the fact that sp^2 bonding (graphite) and not sp^3 bonding (diamond) is the thermodynamically most stable phase of carbon under typical laboratory conditions.[1] In contrast to other semiconductors and insulators, the band gap of diamond (5.5 eV)[2] is of a size usually found only in strongly ionic solids, yet the bonding is completely covalent. These properties bring special interest to the atomic structure and electronic properties of the diamond surface. Because of the dichotomy[3] in Fermi level pinning positions between covalent and strongly ionic (wide band gap) materials in Schottky barriers, this wide band gap covalent material is of particular interest.

We present in this paper studies of the diamond (111) 1 × 1 surface. Recent theoretical work of Ihm *et al.* has shown the ideal unreconstructed diamond (111) surface to have sharp surface states in the fundamental gap.[4] However, in contrast with previous work on the (111) surface of column IV semiconductors in which intrinsic surface states were detected,[5] we find no emission from states in the gap on diamond (111) 1 × 1. This result is in agreement with the recent work of Himpsel *et al.*[6] Over the last two decades, several LEED[7,8,9] studies have been made which indirectly support the thesis that hydrogen terminates the diamond (111) 1 × 1 surface. More recent work demonstrates that the photoelectric threshold occurs at band gap energy radiation and concludes that a negative electron affinity at the surface exists.[6] Our work suggests the presence of hydrogen and confirms the photoelectric threshold at band gap energy radiation but shows the electron affinity at the surface to be positive. Band bending is shown to result in an effective negative electron affinity under certain conditions, and the yield measurements of Himpsel *et al.*[6] are re-evaluated in this light. Evidence for a surface dipole which is sensitive to band gap radiation is presented. In confirmation of our earlier work,[10] we report on the relative cross section of the upper p-like part of the valence band with respect to the lower s-like portion.

II. EXPERIMENTAL

The sample under study is the (111) surface of a type IIa diamond.[11] The diamond (labeled D3) was mechanically polished on a cast iron wheel using 2 μm diamond grit in olive oil. Note that the olive oil may act as a source of hydrogen for the diamond surface during polishing. The surface was polished within 2° of the crystallographic (111) plane (verified by Laue back diffraction) and has a surface area of 4 × 5 mm^2. An ultrasonic rinse in acetone and then alcohol preceded the mounting of the diamond into the vacuum chamber. After a normal (~24 h at 170°C) bakeout, we found, in agreement with earlier results of both Lurie and Wilson[9] and Himpsel *et al.*,[6] a sharp 1 × 1 LEED pattern. Except for the spectra obtained at $\hbar\omega = 160$ eV and $\hbar\omega = 65$ eV, the diamond was swabbed with a cotton applicator dampened with alcohol just before insertion into the vacuum chamber and heated after bakeout for 15 min at 200° to 300°C. This additional step appeared to remove sulphur contamination. The diamond was not exposed to an electron beam (either for AES or LEED studies) until after all photoemission studies were complete, since earlier studies which were performed in our laboratory[12]

 0022-5355/80/051087-07$01.00

and have been confirmed elsewhere[13] indicate that such a beam could produce graphitic carbon. A Physical Electronics Model 255G double-pass CMA was used for electron analysis. Below $\hbar\omega = 65$ eV, a resonance lamp[14] with monochromator[15] using He, Ne, and Ar discharges was used as a light source. Beam line 1-1 at SSRL, equipped with the grasshopper monochromator[16] with a resolution $\Delta\lambda = 0.1$ Å, provided the photon energies from 65 eV through 200 eV. The experimental configuration is such that the CMA is concentric about the sample normal, and the light impinges at glancing incidence 75° from the sample normal. At SSRL, the polarization of the light and the CMA axis lie in the same plane. All work was performed in all-metal vacuum chambers with a base pressure 5×10^{-11} Torr ($\sim 6.6 \times 10^{-9}$ Pa) and working pressures of 5×10^{-10} and 1×10^{-10} Torr ($\sim 6.6 \times 10^{-8} - 1.3 \times 10^{-8}$ Pa), respectively, when the resonance lamp or SSRL was used. A freshly evaporated film of Au was used in all cases to provide a Fermi level reference for the EDC's.

A PEK Model 202 superhigh pressure mercury lamp was employed as a source for band gap radiation. The photon energies of the light from the mercury lamp extend from below the band gap energy (5.5 eV) up to $\hbar\omega \approx 6.5$ eV. A lithium fluoride window (high photon energy cutoff $\hbar\omega_c \approx 11.8$ eV) transmitted the mercury lamp radiation into the chamber and to the sample. The mercury lamp was also used as a source on a McPherson 225 Monochromator for photoelectric yield measurements over the energy range $5.3 \lesssim \hbar\omega \lesssim 6.4$ eV. The photon flux was normalized using a Cs_3Sb photocathode.[17] In these experiments, a LiF window provided vacuum isolation of the sample chamber from the monochromator. The energy resolution was $\Delta E \lesssim 0.05$ eV.

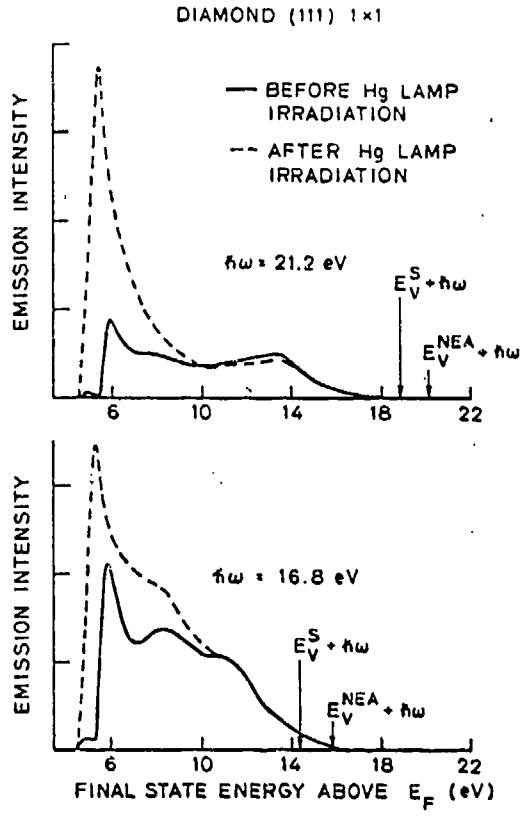

FIG. 1. Exposure to radiation from a mercury lamp source results in a change in electron affinity of the diamond (111) 1 × 1 surface. The EDC's show that the low energy threshold shifts by ~1 eV, while the emission from the valence band remains unaltered in energy position. The figure does not show the full shift due to the low energy acceptance cutoff of the analyzer. Indicated in the figure is the energy position of the valence band maximum at the surface from the band bending model discussed in the text (E_V^S). For comparison, the energy position of the valence band maximum under the assumption of a true negative electron affinity (in the after *Hg* lamp exposure case) is also shown (E_V^{NEA}). The small feature to the left of the "before" EDC's is an artifact of the photoemission light source and electron analyzer configuration.

III. RESULT AND DISCUSSION

A. General results

Characterization of the diamond using Auger electron spectroscopy (electron beam energy = 2 keV, current = 3.5 μA) indicated only minor contamination (typically ≲1 at. % oxygen, <0.5 at. % Si). The carbon Auger peak shape was characteristic of diamond as established by Lurie and Wilson.[18] In the work done at $\hbar\omega = 160$ eV and $\hbar\omega = 65$ eV, a trace of sulfur (≲0.5 at.%) was also detected. The presence of silicon was confirmed by observing the Si 2*p* photoelectron peak ($\hbar\omega = 180$ eV) at ~100 eV binding energy.

Whenever electron spectroscopies are applied to low conductivity materials, the possibility of sample charging exists. On the diamond D3, we found no noticeable sample charging to occur during photoemission. Unlike the results of Lurie and Wilson[9] and others[7,8] but in agreement with Himpsel *et al.*,[6] bright 1 × 1 LEED patterns could be obtained from D3 with primary energies as low as 25 eV. Other diamonds which were studied, for example, D1,[19] would charge 20 eV or more positive during photoemission. It was found that the concurrent application of the mercury lamp radiation (to induce photoconduction) during the photoemission experiment would remove the charging in D1. However, in diamond D3, there were typically no changes in photoemission with the concurrent illumination of the mercury lamp source which would indicate charging. We take this as evidence that sample charging is not a problem with diamond D3 during photoemission.

B. Changes in the electron affinity

1. Results

It appears that the true electron affinity of diamond (111) 1 × 1 surface is sensitive to band gap radiation (see Fig. 1). Photoemission electron distribution curves (EDCs) may be used to measure the electron affinity of solids. Thus, $\chi = \hbar\omega - Eg - W$ where χ is the electron affinity, $\hbar\omega$ is the exciting photon energy, Eg is the band gap energy, and W is the width of the emission in the EDC (from the vacuum level to the valence-band maximum). Through the use of a long wavelength pass filter (Corning No. 7740 Glass, $E_p \approx 3.1$ eV), we found that $\hbar\omega \lesssim 3.1$ eV had no effect on the surface electron affinity while, with no filter, the surface electron affinity is reduced by $\Delta\chi \gtrsim 1.0$ eV after being subject to the full mercury lamp radiation spectrum (which extends past the band gap energy, $Eg = 5.5$ eV, up to $\hbar\omega = 6.5$ eV). The time

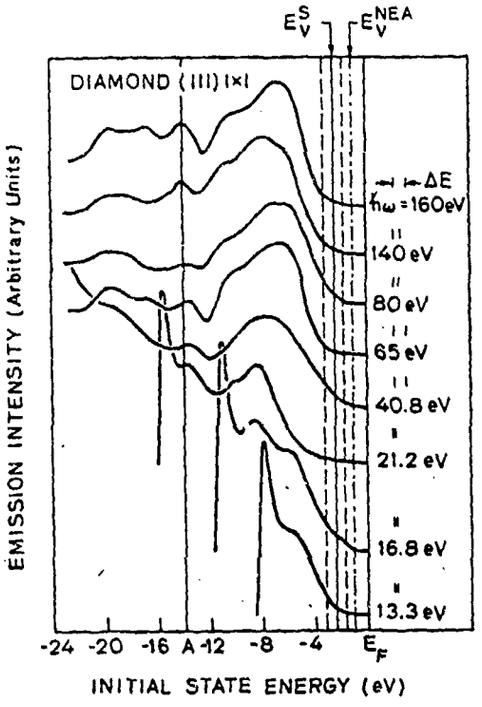

FIG. 2. Electron distribution curves are shown for the photon energies 13.3 eV $\leq \hbar\omega \leq$ 160 eV. A trend in the cross section of the upper (p-like) part of the valence band as compared to the lower (s-like) part of the valence band can be seen. No intrinsic surface state emission from the fundamental gap can be seen. The tailing of the valence band into the band gap is believed to be indicative of band bending. See Fig. 1 for a description of E_V^S and E_V^{NEA}. The dashed lines indicate the range of uncertainty in the determination of E_V^S.

required for the electron affinity to return to its original value is about 5 h at 1×10^{-10} Torr (1.3×10^{-8} Pa). Inspection of Fig. 1 demonstrates the increase in W and therefore the decrease in χ, the electron affinity, due to the exposure to the band gap radiation. Note that those features in the EDC due to direct transitions from the valence band have not noticeably moved in energy position as a function of exposure to the band gap radiation. The optical absorption length at $\hbar\omega = 20$ eV is ~50 Å,[20] and the escape depth of the photoemitted electrons from high in the valence band would be expected to be 20 Å or shorter.[21] The surface dipole layer must therefore exist completely within 5 Å or less of the surface. Otherwise, the dipole's electrostatic fields would extend over a major portion of the sampled region, resulting in a greater shift in the energy distribution of electrons above 10 eV (in Fig. 1) than is observed. These results demonstrate that a surface dipole on the atomic scale is involved and that there is no change in the band bending. In other words, there must be a charge rearrangement at the surface, resulting in a change in surface dipole, with no change in the net amount of surface charge.[22]

One should note that the electron energy analyzer (CMA) has a low energy cutoff (determined by the work function of a grounded screen which covers the entrance aperture) below which no electrons may enter. In experiments where the sample is biased so that the true low energy cutoff from the diamond (after mercury lamp irradiation) can be seen, an estimate of $\Delta\chi \gtrsim 1.0$ eV is determined. The small peak at the left of each "before exposure" EDC is an artifact of the electron analyzer.

2. Discussion

The surface dipole and its sensitivity to the Hg lamp radiation could be explained by the adsorption and desorption of a background gas (such as oxygen or hydrogen) or by a long-lived trap at diamond surface. Adsorption could involve electron transfer to the adatoms from the surface carbon atoms of diamond. This would increase the electron affinity of the solid. If band gap radiation could then cause photon stimulated desorption, the adsorbate-induced charge transfer would be removed and the electron affinity would be lowered. Alternatively, there is a possibility that a long-lived trap which is localized at the diamond surface could be emptied or filled by the Hg lamp radiation. The change in the local charge distribution could then result in changes in the surface electron affinity.

C. Electronic structure of diamond (111) 1 × 1

Results from photoemission experiments over the photon energy range 13.3 eV $\leq \hbar\omega \leq$ 160 eV are shown in Fig. 2. Of special importance is the absence of emission from the fundamental gap. This confirms the results of Himpsel *et al.* in which no intrinsic surface states were found with ionization energies in the gap.[6] The tailing of the emission into the gap (apparent in Fig. 2) is suggestive of a downwards band bending at the surface (see Sec. III.D).

Over the last decade, there have been many calculations of the bulk valence-band structure of diamond.[23–24] In Fig. 3, we compare our measured EDC for $\hbar\omega = 160$ eV (with background removed) to the bulk density of states as calculated by Painter *et al.* using the discrete variational method.[23] In this figure, the central peaks are aligned for comparison. Justification for this method of alignment comes from recognizing that this peak remains dispersionless over a wide

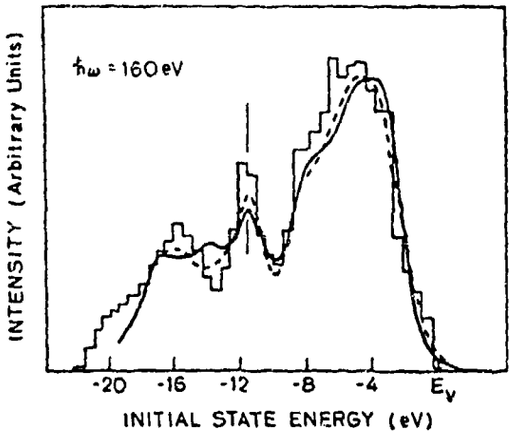

FIG. 3. The density of states for the valence band of bulk diamond (histogram) as calculated by Painter *et al.*[23] is compared to the $\hbar\omega = 160$ eV EDC from two different diamonds. EDC's (with background removed) from the (111) 1 × 1 surface of diamond D1 (solid line) and from the (110) 1 × 1 surface of diamond D3 are shown. Alignment of the valence-band structures was made using the central peak.

TABLE I. Initial state energy positions of features in the EDC's referenced to the Fermi level

$\hbar\omega$ (eV)	A (eV)	B (eV)	C eV)
13.3	...	−2.8	−0.8
16.8	...	−2.6	−0.8
21.2	−13.8	−5.1	−0.7
40.8	−13.6	−2.5	−1.1
65	−13.8	−3.7	−2.2
80	−13.8	−2.6	−1.3
140	−13.9	−3.2	−1.8
160	−14.0	−3.6	−1.3

Column A. The energy position of the set of peaks labeled A in Fig. 2.
Column B. The energy value found by a straight line extrapolation of the maximum slope at the front of the EDC to the base line.
Column C. The highest energy of electrons emitted in a given EDC.

range of photon energies (see Fig. 2 and Table 1). In comparing the valence-band spectra taken using photon energies from 65 to 200 eV, the major trend was a slow variation in the carbon 2*s*-to-2*p* cross section. Previous experimental work has shown that the cross section of the upper 2*p*-like portion of the valence band is enhanced with respect to the lower 2*s*-like portion at $\hbar\omega = 1253$ eV[25] while, at $\hbar\omega = 50$ eV, the situation is reversed.[10] From the close correspondence of the 160 eV spectra to the valence-band density of states, we suggest that the ratio of the carbon 2*s*-to-2*p* cross section is approximately unity at $\hbar\omega = 160$ eV. This cross section result is consistent with that of Bianconi *et al.* in their photoemission study of the valence band of graphite.[26] They found the 2*s*-to-2*p* cross section ratio for graphite to be unity at $\hbar\omega \approx 120$ eV.

D. The band bending model

1. Width of the EDC

The photoemission results indicate that the electron affinity at the surface is positive, both before and after Hg lamp irradiation. Since $\chi = \hbar\omega - Eg - W$, one may measure the emission width W in order to find the electron affinity when both the photon energy and bandgap energy are known. The width W is measured from the low energy cutoff of emission E_l up to the valence band maximum at the surface E_V^S. One should note that while E_l is relatively simple to determine experimentally, E_V^S is difficult to estimate because of tailing of the emission above E_V^S (possibly due to band bending) and because of direct transitions and/or matrix element effects on the EDC. For convenience, let $E_F^S = E_F - E_V^S$ (the surface Fermi level pinning position) denote the energy separation of E_V^S from the Fermi level E_F. Extrapolation of the region of maximum slope of the peak at the top of the valence band emission in the EDC to the baseline gives an estimate of $E_F^S \approx 2.6$ eV (see column B in Table I). Making use of the density-of-states calculation of Painter *et al.*[23] (Fig. 3), an estimate of $E_F^S \approx 2.3$ eV is found. Comparison of the self-consistent calculation of Zunger and Freeman[27] to our results by rescaling the energy scale of the density of states of Painter *et al.* results in an estimate as small as $E_F^S = 1.8$ eV. In further calculations, $E_F^S = 2.3$ eV will be used as a best estimate; however, it should be recognized that this is not a highly accurate estimate ($\sim \pm 0.8$ eV). We find $\chi = 2.3 \pm 0.8$ eV initially and $\chi = 1.3 \pm 0.8$ eV after band gap radiation exposure. The uncertainty in χ is due principally to the uncertainty in the estimate of E_F^S. In any case, the true electron affinity is always positive. This conclusion coupled with the photoelectric threshold at band gap radiation (see Fig. 4) demonstrates the existence of an effective negative electron affinity and suggests a band bending model of the diamond (111) 1 × 1 surface.

2. Photoelectric yield

A three-step model of photoemission may be used to estimate the expected yield from a flat band semiconductor with a real electron affinity which is less than zero.[28,29] One finds $Y(\hbar\omega) = P(\hbar\omega)/[1 + (1/L(\hbar\omega)\,\alpha(\hbar\omega))]$ where Y is the electron yield in electrons per photon, P is the probability for an electron to escape once it has reached the surface (if there is a negative electron affinity at the surface, this should approximate unity and be independent of $\hbar\omega$), L is the electron escape length, and α is the absorption coefficient of the incident light. Note that electron-hole pair production due to electron–electron scattering does not enter into the yield unless $\hbar\omega > 2\,Eg$ and is not included in this model. In Fig. 4, we show for three values of $L(\hbar\omega)$ (100, 1000, 10 000 Å) the calculated yields using the three-step model and assuming $P(\hbar\omega) = 1$. From $\hbar\omega = 5.5$ eV through 6.0 eV, $\alpha(\hbar\omega)$ was obtained from the work of Clark *et al.*[2] Above 6.5 eV, $\alpha(\hbar\omega)$ was derived from the optical constants of Roberts and Walker.[30]

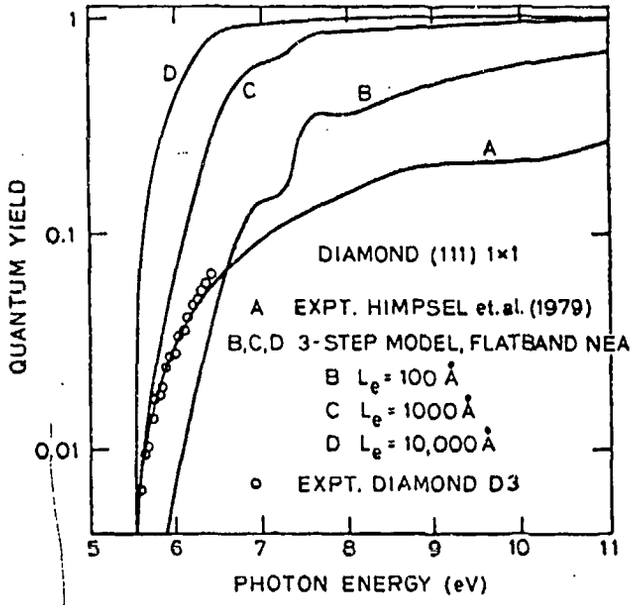

FIG. 4. Comparison of yield measurements on the diamond (111) 1 × 1 surface with calculations of the expected yield in the case of a true negative electron affinity are shown. The experimental results shown are the absolute quantum yield measurements by Himpsel *et al.*[6] (curve A) and relative yield results from diamond D3 which are normalized to the work of Himpsel *et al.* The calculations of yield are made with the three-step model, as described in the text. L_e is the electron escape depth. Comparison of the shapes of calculated vs measured yield indicate the diamond must have a positive electron affinity at the surface while the band gap energy threshold ($Eg = 5.5$ eV) demonstrates the existence of an effective negative electron affinity.

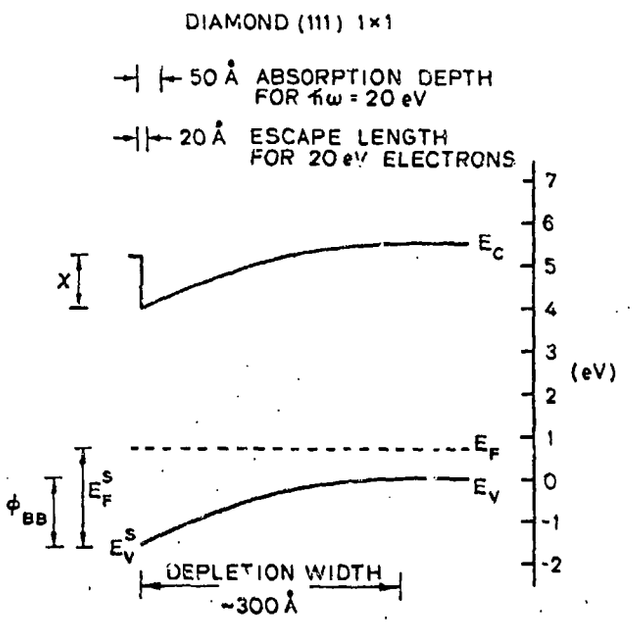

FIG. 5. The band-bending model discussed in the text is illustrated. The symbols are defined as follows: E_F is the Fermi level, E_V is the top of the valence band in the bulk, E_C is the bottom of the conduction band in the bulk, χ is the electron affinity at the surface, E_V^S is the top of the valence band at the surface, E_F^S is the Fermi-level pinning position at the surface which is defined as $E_F^S = E_F - E_V^S$, ϕ_{BB} is the total difference in potential energy due to band bending between the bulk and surface, defined by $\phi_{BB} = E_V - E_V^S$. Note that the total band bending, ϕ_{BB}, is larger than χ, resulting in the vacuum level being lower than the bulk conduction-band minimum, E_C. Therefore, while the electron affinity at the surface is positive, the effective electron affinity, $\chi_{eff} = \chi - \phi_{BB}$, is negative.

Even if $P(\hbar\omega)$ were not unity, it would certainly by expected to be a slowly varying function of $\hbar\omega$. This would result in yield curves of very similar shape to the calculated curves in Fig. 4. Also included in Fig. 4 is the diamond (111) 1 × 1 yield measurement of Himpsel *et al.*[6] to which we have normalized our yield results.

An important result of Fig. 5 is that all of the calculated yield curves (over the wide range of L used) rise much sharper from the photoelectric threshold to $\hbar\omega \simeq 7$ eV than the experimental curve. This sharp rise is characteristic of a true negative electron affinity material and of effective negative electron materials with a very short band-bending length ($\lesssim$30 Å).[28,29] The data is consistent with band bending over a relatively long distance as shown in Fig. 5.

The structure at $\hbar\omega = 7$ to 8 eV in the calculated quantum yield is due to structure in the absorption coefficient.[30] Painter *et al.*, in their band structure calculation of diamond, found similar structure in the joint density of states.[23] Thus, the structure is real and traceable to the electronic structure of diamond. This structure, which is evident in the short ($\lesssim$100 Å) escape length calculations, does not appear in the experimental yield. Also, the experimental yield is not consistent with a sharp saturation in the yield as predicted by the long ($\gtrsim$100 Å) escape length calculations. These results argue against a true negative electron affinity.

A third feature in the yield results of Himpsel *et al.* which is of importance and suggests band bending is not shown in Fig. 5. This is the large dip in the quantum yield occurring at about $\hbar\omega = 20$ eV.[6] This loss in the yield occurs in coincidence with an optical transition from deep in the valence band to low in the conduction band at and near the conduction band minimum near Δ.[31] In light of this, such a dip in yield is well explained by a band-bending model. At $\hbar\omega = 20$ eV, the attenuation length of the light is about 50 Å.[20] Therefore, the absorption of the light occurs totally in the band-bending region where the conduction band minimum is well below the vacuum level (see Fig. 5). The electrons excited to the bottom of the conduction band cannot escape and, hence, the yield drops from its value at either higher or lower $\hbar\omega$ where states near the conduction band minima are not important final states for a dominant direct transition. In the case of a true negative electron affinity, the electrons at the bottom of the conduction band near the surface could escape the solid just as those electrons did escape which were excited upon band gap radiation.[28,29]

3. Description of the band bending model

The results cited in the previous two sections can be adequately explained via a band bending model. Requirements that these results place on the band bending are: (1) the change in electrostatic potential ϕ_{BB} due to band bending must be greater than the true electron affinity. (2) The band bending length must be short enough so that at photothreshold electrons excited to final states above the vacuum level have a finite probability of traversing the band bent region and exiting from the diamond. (3) The band bending length must be long with respect to the electron escape depth at 50 to 150 eV kinetic energy since the valence band maximum in the EDCs indicate a positive electron affinity. (4) The band bending length must be long with respect to the absorption length (~50 Å)[20] at $\hbar\omega = 20$ eV in order to be consistent with the dip in yield discussed in Sec. III.D.2. From these requirements and physical properties of diamond, the band bending model shown in Fig. 4 was developed. Values of interest are (1) the bulk Fermi level E_F measured with respect to the valence-band maxima in the bulk E_V, (2) the Fermi level at the surface $E_F^S = E_F - E_V^S$, (3) the total potential energy difference ϕ_{BB} between the bulk and the surface due to band bending $\phi_{BB} = E_V - E_B^S$, and (4) the depletion width d over which distance the band bending occurs. In Fig. 4, we assume $\phi_{BB} = 1.5$ eV and assume a uniform space charge density of 10^{18} cm^{-3}. The depletion width is $d \approx 300$ Å.[32] Collins and Lightowlers, in their study of type IIb diamonds, found that $N_A \approx 5 \times 10^{16}$ cm^{-3}.[33] This would result in a depletion width $d \lesssim 1500$ Å. Since the electrically active impurity levels in diamond are, in general, found to be deep levels and compensated,[33] the band bending model as developed should be viewed as indicative of the important parameters which determine the band bending and not as the precise shape of the band bending.

4. Emission above E_V^S

A prominent feature in Figs. 1, 2, and 3 is the tailing of emission above the valence band maximum at the surface E_V^S. This emission might be due to inhomogeneities in the diamond, defect or surface states in the band gap, or emission

from nondiamond carbon contamination. However, in our opinion, this emission is indicative of downwards band bending and should be expected when the band bending length is approximately an order of magnitude longer than the photoemission probing depth. In the case of a downwards band bending, the weak emission from the valence band maximum (at a depth of several electron escape lengths) has no competition with the stronger emission from the volume which is closer to the surface. Therefore, emission from deeper in the diamond will form an approximate exponentially decaying tail on the high kinetic energy side of the EDC.

For $13.3 \leq \hbar\omega \leq 160$ eV, pair production (threshold at $\hbar\omega = 11$ eV) probably dominates the energy loss process. Because the energy loss in pair production is about two orders of magnitude (~10 eV) larger than that for electron–phonon scattering (~0.1 eV), pair production will dominate even when the electron–phonon scattering length is shorter than the electron–electron scattering length.[34] The electron scattering length vs electron kinetic energy has not been measured for diamond but can be roughly extrapolated from GaAs[35] and Si.[36] Thus, one would expect it to have a minimum near a kinetic energy of 70 eV with the escape length rising faster as one goes below ~20 eV than on the high energy side of the minimum. Recognizing that the high energy cutoff E_m will be complicated by modulations caused by direct transitions and/or other matrix element effects, we see that the high energy cutoff of the EDC (column C in Table 1) follows the expected trend. Note that the values listed in Table 1 are being referenced to the appropriate initial state energies below the Fermi level. Using Table 1, we find E_m has a minimum of −2.2 eV at 65 eV and rises relatively sharply to a maximum of ~−0.8 eV for the lowest values of photon energy. Column B in Table 1 was obtained by a linear extrapolation down from the point of maximum slope in the EDC. Although this measurement might be expected to be even more sensitive to the effects of direct transitions than E_m (column C), the same general trend is repeated by column B.

Under the assumption that the emission above E_V^S is due to the band bending as described above, an estimate of the energy position of the bulk valence maximum can be made. Because of the short escape depth in comparison to the total band bending length, emission from the bulk valence band (where the bands are becoming flat and the valence band maximum is approaching the bulk valence band maximum value) will not, in general, reach the surface. Therefore, the energy position of the valence-band maximum in the bulk will be, at worst, underestimated if we use the endpoint of this exponentially decaying tail as indicative of the energy position of the bulk valence band maximum. Applying this technique to the EDCs at $\hbar\omega = 13.3$, 16.8, and 21.2 eV (see column C in Table 1), we find that the energy difference between the Fermi level E_F and bulk valence-band maximum E_V is $E_F - E_V \lesssim 0.8$ eV. This would imply that the total band bending is $\phi_{BB} = E_V - E_V^S = 1.5 \pm 0.8$ eV. The effective electron affinity will be given (see Fig. 5) by the true electron affinity χ minus the band bending ϕ_{BB} yielding $\chi_{eff} \lesssim 0.8 \pm 0.2$ eV initially and $\chi_{eff} \lesssim -0.2 \pm 0.2$ eV after band gap radiation exposure.[37] Hence, the effective electron affinity becomes negative after exposure to the mercury lamp radiation.

IV. CONCLUSIONS

Photoemission studies over the photon energy range $5 \leq \hbar\omega \leq 200$ eV were made to study the surface and bulk electronic states of diamond. The apparent cleanliness of the surface (as determined by AES which cannot detect hydrogen), the sharp 1 × 1 LEED pattern, and the LEED *I–V* data of Lurie and Wilson[9] leads one to consider the electronic structure of the ideal unreconstructed diamond surface. Ihm *et al.* found, for such a surface, a sharp surface state ~1.8 eV above the valence-band maxima.[4] Results on other column IV semiconductors have demonstrated the ability of photoemission to detect intrinsic surface states.[5] However, in agreement with Himpsel *et al.*,[6] we find no evidence for surface state emission from the fundamental gap. Although we have no direct evidence for hydrogen contamination, these results suggest the role of hydrogen as a termination to the diamond lattice. An expectation of hydrogen termination for the (111) 1 × 1 diamond surface has been expressed previously by several authors.[7,8,9] Clearly, there exist techniques (low energy electron loss, electron stimulated desorption, photon stimulated desorption, secondary ion mass spectroscopy, etc.) which, when used in conjunction with LEED and photoemission, may be able to resolve this question.

The EDCs above $\hbar\omega = 40$ eV resemble the bulk valence-band density of states. At $\hbar\omega = 160$ eV, the cross section ratio between the upper (2*p*-like) and lower (2*s*-like) part of the valence band appear to be approximately unity. A Fermi level pinning at the surface ($E_F^S = 2.3 \pm 0.8$ eV) due to extrinsic defect or surface states is found. Exposure to bandgap radiation results in a reduced electron affinity ($\Delta\chi \geq 1.0$ eV) at the surface. The effect is tentatively associated with photostimulated adsorption–desorption of a background gas. While the diamond is found at all times to have a positive electron affinity at the surface, after band gap irradiation, the electron affinity is less than the band bending, resulting in an effective negative electron affinity. To summarize our numerical results, we find (1) the bulk valence band is $\lesssim 0.8$ eV below the Fermi level, (2) the Fermi level pinning position at the surface is 2.3 ± 0.8 eV above the valence-band maxima, (3) the electron affinity is 2.3 ± 0.8 eV before exposure to the mercury lamp radiation and 1.2 ± 0.8 eV afterwards, and (4) the effective electron affinity is 0.8 ± 0.2 eV before mercury lamp irradiation and is less than zero afterwards.

ACKNOWLEDGMENTS

The authors would like to express their appreciation to P. M. Stefan, M. L. Shek, D. L. Weissman-Wenocur, and P. Jupiter for their assistance in these experiments. Helpful discussions with Marvin Cohen are gratefully acknowledged. We wish to acknowledge De Beers Industrial Diamond Division and in particular Dr. F. A. Raal of the Diamond Research Laboratory, Johannesburg, South Africa for kindly supplying the diamonds used in this work.

Work was supported by the U.S. Army Research Office under Contract No. DAAG29-78-G-0130. Part of this work was performed at the Stanford Synchrotron Radiation Laboratory which is supported by the National Science Foundation under

Grant No. DMR77-27489 in cooperation with the Stanford Linear Accelerator Center and the Department of Energy.

[a]Stanford Ascherman Professor of Engineering.
[b]Permanent Address: Photon Factory, KEK, Oho-Machi, Tsukuba-Gun, Ibaraki-Ken, 300-32 Japan

[1]G. Muncke, in *The Physical Properties of Diamond*, edited by J. E. Field (Academic, London, 1979), p. 473.
[2]C. D. Clark, P. J. Dean, and P. V. Harris, Proc. R. Soc. London, Ser. A 277, 312 (1964).
[3]S. Kurtin, T. C. McGill, and C. A. Mead, Phys. Rev. Lett. 22, 1433 (1969).
[4]J. Ihm, S. G. Louie, and M. L. Cohen, Phys. Rev. B 17, 769 (1978).
[5]L. F. Wagner and W. E. Spicer, Phys. Rev. Lett. 28, 1381 (1972); D. E. Eastman and W. D. Grobman, Phys. Rev. Lett. 28, 1378 (1972).
[6]F. J. Himpsel, J. A. Knapp, J. A. Van Vechten, and D. E. Eastman, Phys. Rev. B 20, 624 (1979).
[7]J. B. Marsh and H. E. Farnsworth, Surf. Sci. 1, 3 (1964).
[8]J. J. Lander and J. Morrison, Surf. Sci. 4, 241 (1966).
[9]P. G. Lurie and J. M. Wilson, Surf. Sci. 65, 453 (1977).
[10]P. E. Gregory, I. Lindau, and W. E. Spicer, Bull. Am. Phys. Soc. 21, 1314 (1976).
[11]The diamond D8, obtained from De Beers Diamond Research Laboratory, Johannesburg, was classified by De Beers as a type IIa diamond. Note that while type IIb diamonds are, by definition, semiconducting diamonds, the classification type IIa includes diamonds with relatively low resistivity, although most IIa diamonds are insulators with very high resistivities. See, for example, R. W. Ditchburn and J. F. H. Custers, in *The Physical Properties of Diamond*, edited by R. Berman (Clarendon Press, Oxford, 1965), p. 1; *Properties of Diamond* (obtainable from De Beers Industrial Diamond Division, Sunninghill, Ascot, Berkshire SL59PX England).
[12]B. B. Pate, T. Ohta, I. Lindau, and W. E. Spicer, presented at 6th Annu. Meet. SSRL Users Group, 1979; abstract in SSRL Report No. 79/05.
[13]F. J. Himpsel and D. E. Eastman, these proceedings (PSCI-7, February 1980).
[14]K. Yu (Ph.D. thesis, Stanford University, 1976).
[15]J. N. Miller (Ph.D. thesis, Stanford University, 1979).
[16]F. C. Brown, R. Z. Bachrach, and N. Lien, Nucl. Instrum. Methods 152, 73 (1978).
[17]The Cs_3Sb photocathode used is our standard cell #126 which has a calibration traceable to the National Bureau of Standards.
[18]P. G. Lurie and J. M. Wilson, Surf. Sci. 65, 476 (1977).
[19]Diamond D1, type IIb, was obtained from De Beers; exhibits a blue coloration. A mechanically polished (110) surface was studied.
[20]See the absorption coefficient data in Ref. 6, which was derived from the optical constants in Ref. 30.
[21]I. Lindau and W. E. Spicer, J. Electron Spectrosc. Relat. Phenom. 3, 409 (1974).
[22]In this case, surface charge is meant to include all charge within 5 Å of the physical surface.
[23]G. S. Painter, D. E. Ellis, and A. R. Lubinsky, Phys. Rev. 4, 3610 (1971).
[24]A. M. Stoneham, in *The Properties of Diamond*, edited by J. E. Field (Academic, London, 1979), p. 185.
[25]F. R. McFeeley *et al.*, Phys. Rev. B 9, 5268 (1974).
[26]A. Bianconi, S. B. M. Hagström, and R. Z. Bachrach, Phys. Rev. B 16, 5543 (1977).
[27]A. Zunger and A. J. Freeman, Phys. Rev. B 15, 4716 (1977).
[28]W. E. Spicer and R. L. Bell, Astron. Soc. Pac. Leafl. 84, 110 (1972), and references therein.
[29]W. E. Spicer, Appl. Phys. 12, 115 (1977).
[30]R. A. Roberts and W. C. Walker, Phys. Rev. 161, 730 (1967).
[31]See band diagrams in Ref. 23.
[32]Downwards band bending in a p-type diamond by 1.5 eV falls into the depletion regime as discussed in Chap. 9. S. M. Sze, *Physics of Semiconductor Devices* (Wiley, New York, 1969).
[33]A. T. Collins and E. C. Lightowlers, in *The Properties of Diamond*, edited by J. E. Field (Academic, London, 1979), p. 79.
[34]R. N. Stuart, F. Wooten, and W. E. Spicer, Phys. Rev. Lett. 10, 7 (1963).
[35]P. Piannetta *et al.*, Phys. Rev. B 18, 2792 (1978).
[36]C. M. Garner *et al.*, Phys. Rev. B 19, 3944 (1979).
[37]The important measurements concerning the value of the effective electron affinity or the energy difference between the bulk conduction-band minimum and the vacuum level is determined experimentally independent of the energy position of the valence-band maximum at the surface. Simply put, the effective electron affinity is given by $\chi_{eff} = \hbar\omega - W - Eg$ where W, in this case, is the total width of emission in the EDC—that is, from the low energy cutoff E_l up to the cutoff of emission from the bulk valence band. The photon energy $\hbar\omega$ when the resonance lamp is used and the band gap Eg are both known to a high degree of accuracy (± 0.05 eV or better). The width W is well determined also. The low energy cutoff can be measured ±0.1 eV, and the high energy cutoff is given by the valence-band maximum in the bulk; it was found to be $E_V \leq E_F - 0.8$ eV. The result we find (after band gap radiation exposure) is $\chi_{eff} \leq -0.2 \pm 0.2$ eV.

Formation of surface states on the (111) surface of diamond[a)]

B. B. Pate, P.M. Stefan, C. Binns,[b)] P. J. Jupiter, M. L. Shek, I. Lindau, and W. E. Spicer[c)]

Stanford Electronics Laboratories, Stanford University, Stanford, California 94305

(Received 3 April 1981; accepted 24 June 1981)

Experimental studies of the diamond (111) surface are presented. While no intrinsic surface states have been found on the 1×1 surface, our new results in ultraviolet photoemission spectroscopy ($15\ \text{eV} \lesssim h\nu \lesssim 25\ \text{eV}$) show evidence of a band of surface states on the $2\times2/2\times1$ reconstructed surface. The band of surface states (with an integrated emission on the order of one filled state per surface atom) is centered at 2.5 eV below the Fermi level (1.1 eV below the valence-band maximum). The band width is 1.8 eV FWHM. In the case of the $2\times2/2\times1$ surface structure, the downwards band-bending is greater by 0.75 eV and the electron affinity is greater by 1.4 eV over the respective values for the 1×1 surface. These new studies necessitate a quantitative revision of our band-bending model [J. Vac. Sci. Technol. 17, 1087 (1980)], although no change in basic concept is required. Preliminary photon-stimulated desorption (PSD) results over the photon energy range $h\nu = 18$–35 eV find hydrogen on the 1×1 surface. This surface hydrogen (possible in the form of hydroxide) may explain the absence of surface states on the diamond (111) 1×1 surface.

PACS numbers: 73.20.Cw, 79.60.Eq

I. INTRODUCTION AND SUMMARY

In this paper, our present state of understanding of the diamond (111) surface is presented. The aspects of the surface which are addressed include (1) the electronic structure, (2) the atomic structure, and (3) the effect of termination of the lattice by foreign atoms. Interest in diamond is stimulated by both its similarity (bulk crystal structure, 100% covalent bonding) and diversity [wide band gap (~5.5 eV), sp^2 stability of graphite] to other elemental (and compound) semiconductors. Himpsel *et al.*[1] suggested that the 1×1 low energy electron diffraction (LEED) pattern coupled with photoemission electron spectroscopy (PES) and Auger electron spectroscopy (AES) results indicated that the diamond (111) 1×1 surface may be an atomically clean, unreconstructed surface. However, photoemission associated with intrinsic surface states was not found. Emission from intrinsic surface states would be expected from a clean unreconstructed surface in consideration of work with other semiconductors[2] and from the specific theoretical work of Pugh[3] and, more recently, Ihm *et al.*[4] We report photon-stimulated desorption (PSD) results which find hydrogen on the 1×1 surface. As noted by Cohen,[5] a monolayer of hydrogen contamination on an otherwise clean and unreconstructed surface would remove the intrinsic surface states from the gap and r ain the 1×1 surface unit cell. Lander and Morrison[6] found that annealing the (111) 1×1 surface in high vacuum at ~1000°C results in a $2\times2/2\times1$ LEED pattern. (Note that, from LEED symmetry alone, a 2×2 structure vs three orientations of a 2×1 structure are indistinguishable; therefore, the structure is identified as $2\times2/2\times1$). We have found, after a similar anneal, that the change in surface structure is concurrent with the formation of a pronounced peak in the photoemission electron-distribution curve (EDC) at 2.5 eV below the Fermi level. While observation of surface state emission in PES from the $2\times2/2\times1$ surface has been recently reported,[7] we report for the first time the energy position, width, and relative intensity of the surface state band emission. The observed surface states on the $2\times2/2\times1$ surface are much broader and fall at a higher binding energy than those states predicted for an ideal unreconstructed 1×1 surface.[3,4] This difference is not surprising (since the atomic surface structures are different in the two cases), but it does suggest the need for theoretical studies of the electronic structure of the reconstructed diamond surface. Our new PES data from 1×1 and $2\times2/2\times1$ surfaces suggest specific changes from our previous estimates regarding the extent of band-bending on the (111) 1×1 surface. However, no substantial changes in the basic concept of our band-bending model[8] is needed.

II. EXPERIMENTAL

Unless otherwise noted, experimental results discussed here are from work on the (111) surface of a type IIb diamond (denoted D4).[9] The sample was mechanically polished and cleaned by the usual method[8] before each experiment. Photoemission measurements were made in a previously described[8] ultrahigh vacuum system utilizing a double-pass CMA electron energy analyzer (energy resolution $\Delta E \simeq 0.2$ eV) and with a base pressure of 5×10^{-11} Torr [6.7×10^{-9} Pa (working pressure ~1×10^{-10} Torr)].

In this chamber, samples were mounted in platinum foil suspended by a single platinum wire. Heating up to 700°C could be accomplished via thermal radiation from a tungsten filament suspended directly behind the sample. Electron bombardment heating (up to and exceeding 1100°C) could be accomplished by applying a positive bias to the sample. Temperature measurements were made using chromel–alu-

 0022-5355/81/030349-06$01.00

mel thermocouples spot-welded to the platinum support in intimate contact to the diamond substrate. The absolute accuracy of the temperature measurement is not expected to be very good, but is used as a reproducible indicator of the true sample temperature. PSD measurements were made in a separate vacuum system with a time-of-flight ion detector as described by Knotek *et al.*[10] and a working pressure of $\sim 2 \times 10^{-9}$ Torr (2.7×10^{-7} Pa).

The PSD chamber was equipped with radiative sample heating by means of a tungsten filament encased in the sample mounting block. The maximum mounting block temperature (~700°C) was not sufficiently high to cause reconstruction of the diamond (111) 1 × 1 surface. The light source in all experiments was beam-line 1-2 at SSRL which is equipped with a Seya–Namioka monochromator. All experiments were performed at a wavelength resolution of $\Delta\lambda = 2.5$ Å (energy resolution ranges from $\Delta E = 0.12$ eV at $h\nu = 25$ eV to $\Delta E = 0.05$ eV at $h\nu = 15$ eV). Normalization to the photon flux was obtained using the photoyield from sodium salycilate.[11] Typically, AES measurements (which are not sensitive to hydrogen) show that the primary contaminant on the diamond (111) surface is oxygen. After a heat-cleaning anneal at 500°C, the oxygen peak-to-peak vs carbon peak-to-peak ratio is 0.04 (~5% monolayer).[12] After a ~950°C anneal, during which the diamond surface reconstructs to the 2 × 2/2 × 1 structure, the oxygen has decreased by an order of magnitude (oxygen-to-carbon AES peak-to-peak ratio 0.003, ~0.5% monolayer). Due to the potential of electron-beam stimulated alteration of the surface,[8] AES and LEED were performed only after all PES measurements were complete. A piece of highly oriented pyrolytic graphite (HOPG)[13] was studied for comparison purposes. The sample was cleaved in air using the "scotchtape" method and then annealed in ultrahigh vacuum to 500°C. AES measurements showed no detectable impurities.

III. DISCUSSION AND RESULTS

A. The formation of surface states

Two groups[1,8] have reported ultraviolet photoemission studies which indicate that there are no filled intrinsic surface states on the diamond (111) 1 × 1 surface (see, for example, Figs. 1 and 2). If the surface were atomically clean, the observed 1 × 1 LEED pattern would indicate an unreconstructed surface. In such a case, the theoretical calculations of Pugh[3] and Ihm *et al.*[4] would predict a sharp, filled surface state in the band gap. According to Cohen,[5] relaxation effects would have little effect on this basic result. He therefore proposed the experimental surfaces are nonideal and may be terminated with hydrogen. While AES is clearly unable to detect hydrogen (except possibly through an interatomic Auger decay), it would appear (in comparison to hydrogen on silicon[14]) that PES should be able to detect as much as a monolayer of hydrogen. Structure associated with hydrogen on diamond has either not been seen or not correctly identified (a dispersionless peak is found at ~12 eV below the Fermi level[7,8] and may be due to hydrogen). Experiments demonstrating the existence of hydrogen (perhaps in the form of OH)

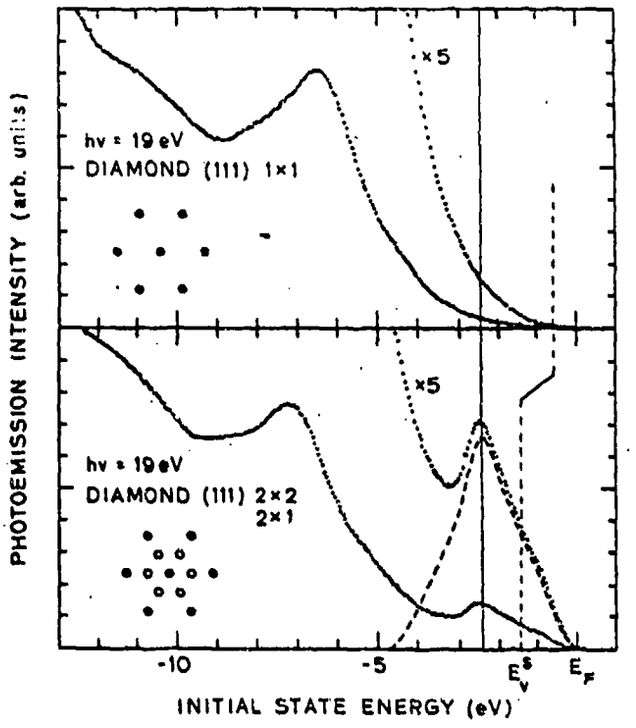

FIG. 1. Photoemission at $h\nu = 19$ eV is shown for both the diamond (111) 1 × 1 surface and the diamond (111) 2 × 2/2 × 1 surface. A typical LEED pattern ($E_p \sim 65$ eV) is shown. Unlike the diamond (111) 1 × 1 surface, the diamond (111) 2 × 2/2 × 1 surface shows evidence of a band of intrinsic surface states. Note that downward band-bending has increased by ~0.75 eV in the case of the 2 × 2/2 × 1 surface. The valence band maximum at the surface (E_V^S) is indicated by the dashed line.

on the diamond (111) 1 × 1 surface are discussed in Sec. III.B.

Similar to the results of Lander and Morrison,[6] we find that upon annealing the (111) 1 × 1 surface for 5 min at ~950°C (background pressure during anneal $\lesssim 4 \times 10^{-9}$ Torr), the surface reconstructs to a 2 × 2/2 × 1 structure. Unlike the (111) 1 × 1 surface, surface states are found on the (111) 2 × 2/2 × 1 reconstructed surface. Shown in Fig. 1 is a comparison between the PES results ($h\nu = 19$ eV) of the 1 × 1 surface and of the 2 × 2/2 × 1 surface. Shown also is a schematic of the LEED pattern as it appears at an electron-beam energy $E_p = 65$ eV. The 1 × 1 and 2 × 2/2 × 1 LEED patterns were seen at all primary beam energies studied ($30 \text{ eV} \leq E_p \leq 150$ eV). Readily apparent in Fig. 1 is the strong emission due to a band of intrinsic surface states on the 2 × 2/2 × 1 surface. The emission is centered 2.5 eV below the Fermi level with a width of 1.8 eV FWHM. In addition to the formation of surface states, Fig. 1 shows an increased downwards band bending of 0.75 eV upon the 1 × 1 to 2 × 2/2 × 1 transition. This result, coupled with a low energy emission threshold which has increased by ~0.65 eV (not shown), signifies an electron affinity increase of ~1.4 eV (see Sec. III.C. for further discussion). In Fig. 2, one can see the relatively dispersionless surface state emission features on the 2 × 2/2 × 1 surface as compared to the dispersion shown in the conduction and valence band direct transition structures from the 1 × 1 surface. Also in Fig. 3, the dispersionless nature of the surface state peaks is ap-

parent. The structure at $h\nu = 15$ eV and at 22 eV $\leq h\nu \leq 25$ eV in the photoemission from the 1 × 1 surface have been previously identified by Himpsel *et al.*[15] (using angle-resolved constant initial-state spectroscopy) as transitions from $\Gamma_{25'} \rightarrow$ "4th" conduction band and $\Gamma_{25'} \rightarrow$ "5th" conduction band, respectively. Although unresolved in their study, their results suggested that there may be another band near the 5th conduction band. Our results (23 eV $\leq h\nu \leq$ 25 eV) on the 1 × 1 surface (Fig. 2) show more clearly the existence of two adjacent conduction bands as predicted by Ihm *et al.*[4] Also shown in Fig. 2 is photoemission from the valence band of highly oriented pyrolytic graphite (HOPG).[13] Evans and James[16] found using transmission electron microscopy that, in the initial stages of graphite growth on the diamond (111) surface, the *c*-axis of the graphite aligns with the [111] direction in the diamond substrate. A question arises as to whether the emission we associated with surface states is instead indicative of a graphitized surface. Therefore, it is of interest to compare the photoemission from the graphite (with the *c*-axis oriented along the surface normal) to the photoemission from diamond (111) 2 × 2/2 × 1 (Fig. 2). The structure in graphite at an initial state energy of ~ −3.0 eV is due to emission from the $\pi 2p_z$ band.[17,18] Note that the binding energy for the graphite $\pi 2p_z$ is about 0.5 eV more than for the diamond (111) 2 × 2/2 × 1 surface state emission and that there is dispersion and much greater modulation of the peak height for the graphite $\pi 2p_z$ peak than the surface state on diamond 2 × 2/2 × 1. Not shown in Fig. 2 is a large conduction band emission peak in graphite, which was first described by Willis *et al.*[19] This emission, which is observed at 7.7 eV above the Fermi level, is not seen in the photoemission from the diamond 2 × 2/2 × 1 surface.

One may roughly estimate the relative strength of the surface state emission so that the number of filled states contributing to the emission can be counted. In order to do this, a basic assumption which we make is that the average matrix elements for the valence band emission are equal to the average matrix elements for the surface band emission. Specific assumptions we make are that the emission in the $h\nu = 19$ eV spectrum (Fig. 1) from −10 to −5 eV initial state energy is 5/21 of that from the entire valence band (width 21 eV) and that the escape length for the emitted electrons in the above distribution (with a kinetic energy of ~10 eV above the conduction-band minima) is ~20 Å. In this case, the expected

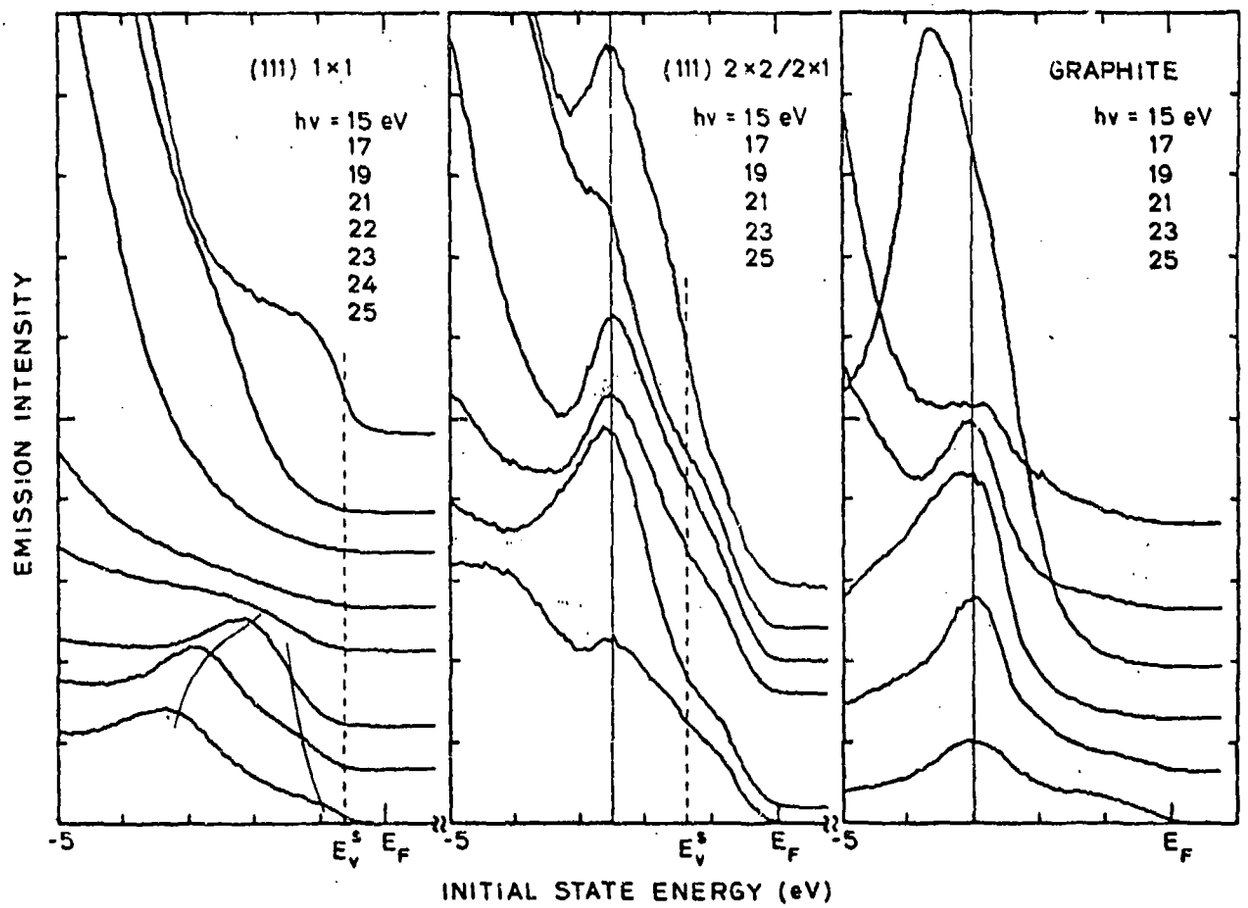

FIG. 2. Comparison is made between the electronic structure at the diamond (111) 1 × 1 surface, the diamond (111) 2 × 2/2 × 1 surface, and the surface (air cleave followed by UHV 500°C anneal) of graphite (HOPG). Note that the surface state band emission on the 2 × 2/2 × 1 surface (center) are dispersionless with energy and have a binding energy about 0.5 eV larger than for the $\pi 2p_z$ band of graphite (right). Also note the splitting of the peak at 23 eV $\leq h\nu \leq$ 25 eV in the emission from the 1 × 1 surface. This is due to two adjacent conduction bands as described in the text. The combined energy resolution of the monochromator and electron detector is ~0.2 eV. For each of the three surfaces studied, the relative intensity of the spectra has been normalized to sodium salicylate photoyield. However, the relative intensity of emission from one surface is not normalized with the emission from a different surface. The dashed line indicates the valence band maximum at the surface (E_v^s).

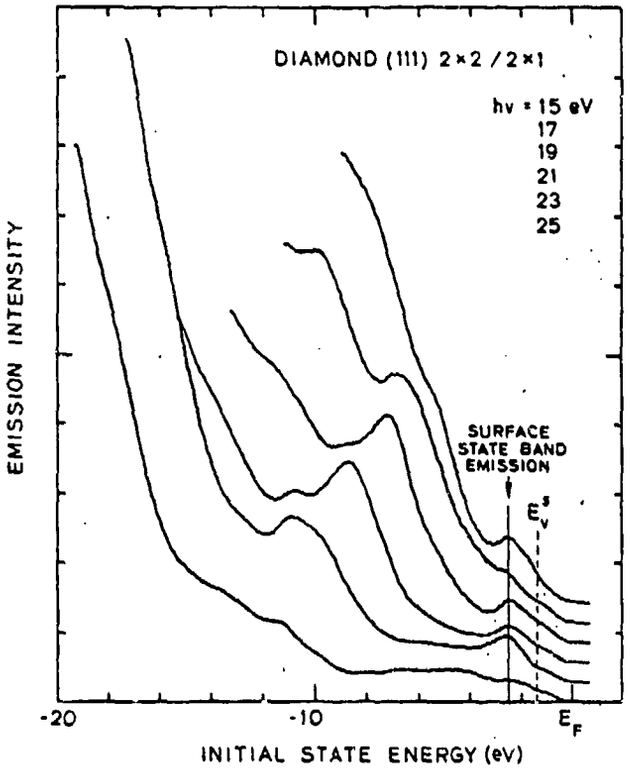

FIG. 3. Photoemission spectra from the diamond (111) $2 \times 2/2 \times 1$ surface is shown over the photon energy range $15\ \text{eV} \leq h\nu \leq 25\ \text{eV}$. Both surface state emission and bulk valence band direct transitions are seen. The spectra are normalized with respect to sodium salicylate photoyield. The energy position of the valence band maximum at the surface (E_v^s) is denoted by the dashed line.

surface state emission intensity for one filled surface state per surface atom is given by

$$I_s = \frac{21}{5} I_v * \frac{N_s}{4\lambda N_v},$$

where I_s is the expected integrated emission intensity for one surface state per surface atom, I_v is the integrated valence band emission intensity from -10 to -5 eV, (21/5) is the ratio of the total valence band width (21 eV) to the valence-band emission width which is used in the calculation (5 eV), λ is the electron escape length appropriate for the valence-band emissions, N_s is the number density of surface atoms, N_v is the number density of bulk atoms, and the factor 4 reflects the number of valence electrons per atom. The predicted intensity ratio in the case of one surface state per surface atom is $I_s/I_v = 0.05$. The actual ratio of emission intensities (at $h\nu = 19$ eV) is 0.09. Similar results were found at other photon energies (e.g., $h\nu = 21$ eV, $I_s/I_v = 0.09$; $h\nu = 23$ eV, $I_s/I_v = 0.05$; $h\nu = 25$ eV, $I_s/I_v = 0.17$). We conclude that there is on the order of one filled surface state per surface atom, although one should recognize that high accuracy can not be expected from this calculation because of the various assumptions made.

B. Evidence for the hydrogenation of the 1 × 1 surface

We have applied the technique of photon stimulated desorption (PSD) to the diamond (111) 1 × 1 surface. Due to sample heating limitations in the PSD chamber (see Sec. II), the $2 \times 2/2 \times 1$ surface was not studied. These preliminary results demonstrate the existence of hydrogen on the (111) 1 × 1 surface. We find the H^+ ion desorption yield to increase slowly from a threshold near $h\nu = 18$ eV and peak at $h\nu \approx 25$ eV. H^+ was the only species found in the time-of-flight mass spectrum. Similar results were found immediately after bakeout and after a 700°C anneal (background pressure during anneal was $\lesssim 5 \times 10^{-8}$ Torr). Exposure to 30 Langmuir (5 min at 1×10^{-7} Torr) deuterium resulted in no detectable PSD of D^+ (or D_2^+) and left the PSD H^+ spectrum unchanged. While the PSD results are definitive evidence as to the presence of hydrogen, the question as to chemical nature (or bonding) of the hydrogen and the concurrent question as to the necessity of the hydrogen to the formation and stability of the 1 × 1 surface remain unresolved. In the remainder of this section, possible explanations for the observed PSD yield are discussed.

Using x-ray stimulated Auger studies of various hydrocarbons, Kelber *et al.*[20] have observed a two-hole final state which is localized at the carbon–hydrogen bond. They have determined the hole–hole repulsion energy experimentally to be 13.6 ± 4 eV. A two-hole localized state at the C–H bond would be expected to break the bond (since both bonding electrons have been ejected) and give rise to H^+ desorption. If such a process were to occur, a hydrogen desorption threshold would be expected at an energy equal to the hole–hole repulsion energy plus twice the one-electron ionization energy of an electron participating in the C–H bond. In the case of silicon, photoemission studies[21] have shown that structures in the valence band photoemission associated with hydrogen (i.e., Si–H bond) occur at ~6 eV below the valence band maximum. Theoretical and experimental (PES) work on the electronic structure of polyethylene has found a similar result for the binding energy of electrons in the C–H bond.[22] If a similar binding energy occurred for electrons in the C–H bond on diamond, then the one-electron ionization energy of those electrons would be ~11 eV for electrons ejected into the diamond conduction band (although, empty surface states in the gap may allow for a smaller first ionization potential). The formation of a two-hole final state would first be energetically possible at $h\nu = (2 \times 11\ \text{eV}) + 13.6\ \text{eV} \approx 36$ eV. It would therefore appear from this model that a two-hole final state desorption process is energetically forbidden in the energy range studied. However, it is clear that further studies are needed to verify the hole–hole repulsion energy and one electron ionization potential for the electrons involved in hydrogen bonding to diamond.

The possibility exists that some or all of the desorbed hydrogen results from the rupture of a hydroxide species rather than a C–H (i.e., diamond–H) bond. AES results show that oxygen is present on the surface in small amounts (<5% ML).[12] The KF[23] Auger decay theory (see below) of PSD predicts a desorption threshold for H^+ ions from hydroxide at the oxygen 2*s* ionization energy (near $h\nu = 20$ eV). Previous observation of H^+ desorption from hydroxide[24] is comparable to our data shown in Fig. 4. However, hydrogen ion yield due to KF PSD from hydroxide has been found to be accompanied by a similar OH^+ yield.[24,10] We report no evidence of de-

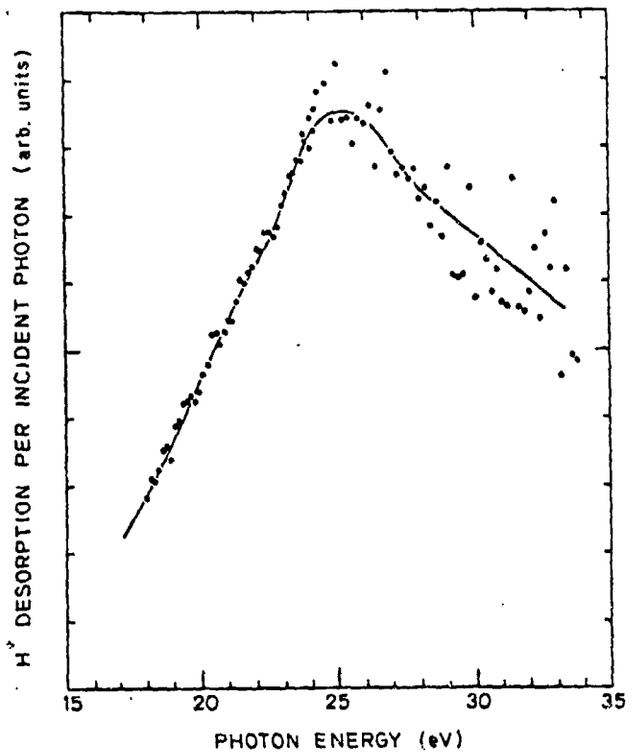

FIG. 4. Hydrogen ion (H^+) photodesorption fom diamond (111) 1 × 1 as a function of photon energy is shown. The ion yield has been normalized to the photon flux by using sodium salicylate photoyield.

sorption of any positively charged species other than H^+ over the photon energy range from 5–35 eV (although it should be noted that the OH^+ yield would be substrate-dependent). To summarize, these preliminary results demonstrate the existence of hydrogen at the diamond (111) 1 × 1 surface but do not conclusively show the chemical form of the hydrogen.

Knotek and Feibelman (KF) have recently proposed a core-hole Auger decay theory of PSD.[23] When the KF theory is operative, PSD can be a powerful adsorbate specific, site specific probe of surfaces. The bonding site selectivity is enhanced by using core levels well spaced in binding energy so that overlap of PSD thresholds which are due to two different desorption channels is avoided. In addition, KF PSD is reported to have an enhanced sensitivity to hydrogen.[10] A more definitive experiment in which hydrogen desorption may be observed via KF PSD (in which ionization of the C 1s level occurs) is presently under way.[25]

C. Band bending

Comparison of the energy position of the photoemission peaks from the 1 × 1 (Fig. 5) and 2 × 2/2 × 1 (Fig. 3) surfaces shows that, upon the formation of surface states on the (111) surface of diamond, there is a uniform shift (~0.75 eV) of the peaks to higher binding energy. The shift in energy position signifies an increase in the downwards band-bending at the surface. The uniformity of the energy shift (0.75 eV ± 0.1 eV) indicates that the band-bending length is rather long with respect to the varying escape length (as a function of final state energy) of the electrons involved (≤30 Å). Our previous estimate of the band-bending length (~300 Å) is consistent with this result. Not shown in the figures is the result that the low kinetic energy cutoff of the electron distribution curves (EDC) from the diamond increases by 0.65 eV (±0.1 eV) upon reconstruction from the 1 × 1 to the 2 × 2/2 × 1 surface structure. This result coupled with the change in band-bending imply that the electron affinity of the 2 × 2/2 × 1 surface is 1.4 eV (±0.2 eV) greater than that for the 1 × 1 surface.

As we have discussed previously,[8] but in contrast to the conclusions of Himpsel *et al.*,[1] the dependence of total electron yield on photon energy (e.g., band gap threshold) and the photoemission electron distributions from diamond (111) 1 × 1 are consistent with and explained by a band-bending model employing a positive electron affinity. Our new results do not alter this conclusion, although certain numerical corrections to our original model are required. While the present work was done on sample D4,[9] previously reported work[8] used sample D3.[9] Results from the two samples are nearly identical except that the low energy threshold and valence band position of diamond D4 (1 × 1 surface) falls at 0.2 eV higher energy than in the case of D3 (1 × 1 surface).

A major numerical change in the estimate of the valence band maximum position with respect to the Fermi level at the (111) 1 × 1 surface is required. We now find (Fig. 2) that the valence band position of the 1 × 1 surface (diamond D4) is ~0.6 eV below the Fermi level. Previously, our estimate was 2.1 eV ± 0.8 eV.[26] These corrections set the true electron affinity on the 1 × 1 diamond surface to a value close to zero. The large error in the initial study was due to a selection of

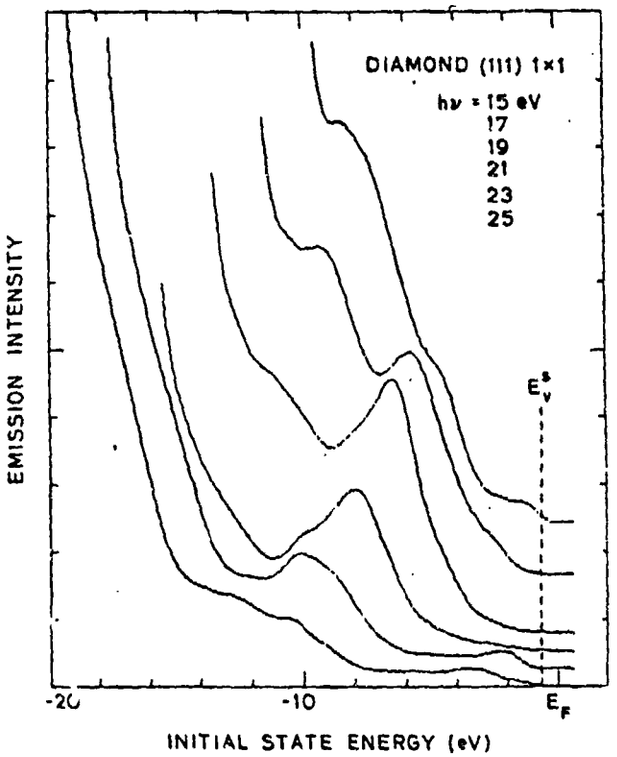

FIG. 5. Photoemission spectra from the diamond (111) 1 × 1 surface is shown over the photon energy range 15 eV ≤ $h\nu$ ≤ 25 eV. The spectra are normalized with respect to sodium salicylate photoyield. The dashed line indicates the energy position of the valence band maximum at the surface.

photon energies which did not contain direct transition emission from the valence band maxima. In our new, more complete study, direct transitions which originate at or near the valence band maximum are seen (see Fig. 2 and Sec. III.B).

ACKNOWLEDGMENTS

Special thanks to F. A. Raal of the DeBeers Diamond Research Laboratory, Johannesburgh, South Africa, for kindly providing the natural diamonds used in this work. The authors express their appreciation to M. L. Knotek for allowing the use of his equipment and beam time during the PSD experiment and to G. Lubriel, J. Kelber, and B. Keol for their help in performing the PSD experiment. The competent design and construction of specialized equipment by Jack McGowan and Phil McKernan of the Stanford Tube Lab is much appreciated.

[a]Work was supported by the U.S. Army Research Office under Grant No. DAAC29-78-G-0130. The experimental work was performed at the Stanford Synchrotron Radiation Laboratory which is supported by the National Science Foundation under Grant No. DMR77-27489 in cooperation with the Standard Linear Accelerator Center and the Department of Energy.

[b]Permanent address: Department of Physics, University of Leicester, Leicester, England

[c]Stanford Ascherman Professor of Engineering

[1]F. J. Himpsel, J. A. Knapp, J. A. Van Vechten, and D. E. Eastman, Phys. Rev. B 20, 624 (1979).

[2]L. F. Wagner and W. E. Spicer, Phys. Rev. Lett. 28, 1381 (1972); D. E. Eastman and W. D. Grobman, Phys. Rev. Lett. 28, 1378 (1972).

[3]D. Pugh, Phys. Rev. Lett. 12, 390 (1964).

[4]J. Ihm, S. G. Louie, and M. L. Cohen, Phys. Rev. B 17, 769 (1978).

[5]M. L. Cohen, Phys. Rev. B 22, 1095 (1980).

[6]J. J. Lander and J. Morrison, Surf. Sci. 4, 241 (1966).

[7]F. J. Himpsel, D. E. Eastman, and J. F. van der Veen, J. Vac. Sci. Technol. 17, 1085 (1980).

[8]B. B. Pate, W. E. Spicer, T. Ohta, and I. Lindau, J. Vac. Sci. Technol. 17, 1087 (1980), and references therein.

[9]The diamonds used in these experiments were natural diamonds obtained from De Beers Industrial Diamond Division, Diamond Research Laboratory, Johannesburg, South Africa. Diamond D4 was classified by De Beers as a type IIb diamond. Diamond D3 was classified as a type IIa diamond.

[10]M. L. Knotek, V. O. Jones, and V. Rehn, Surf. Sci. 102, 566 (1981).

[11]J. A. R. Samson, *Techniques of Vacuum Ultraviolet Spectroscopy* (Wiley, New York, 1967), p. 214.

[12]Monolayer coverages of oxygen on diamond are calculated from AES peak-to-peak ratios assuming a 10 Å escape depth for the C Auger peak and the relative Auger sensitivity (E_p = 3 keV) from L. E. Davis *et al.*, *Handbook of Auger Electron Spectroscopy* (Physical Electronics Industries, Eden Prairie, Minnesota, 1976), p. 13.

[13]Union Carbide highly oriented pyrolytic graphite (HOPG) grade ZYB with a mosaic spread 0.8° ± 0.2° FWHM.

[14]K. C. Pandey, T. Sakuri, and H. D. Hagstrum, Phys. Rev. Lett. 35, 1728 (1975); J. E. Rowe and H. Ibach, Surf. Sci. 43, 481 (1974); T. Sakuri and H. D. Hagstrum, Phys. Rev. B 12, 5349 (1975).

[15]F. J. Himpsel, J. F. van der Veen, and D. E. Eastman, Phys. Rev. B 22, 1967 (1980).

[16]T. Evans and P. F. James, Proc. R. Soc. (London) Ser. A 277, 260 (1964), and references therein.

[17]R. F. Willis, B. Fitton, and G. S. Painter, Phys. Rev. B 9, 1926 (1974).

[18]P. M. Williams, P. Latham, and J. Wood, J. Electron Spectrosc. Relat. Phenom. 7, 281 (1975).

[19]R. F. Willis, B. Feuerbacher, and B. Fitton, Phys. Lett. 34A, 231 (1971).

[20]J. Kelber, R. R. Rye, G. C. Nelson, and J. E. Houston (to be published).

[21]K. C. Pandey, T. Sakurai, and H. D. Hagstrum, Phys. Lett. 35, 1728 (1975); H. Ibach and J. E. Rowe, Surf. Sci. 43, 481 (1974); T. Sakurai and H. D. Hagstrum, Phys. Rev. B 12, 5349 (1975).

[22]J. Delhalle, J. M. Andre, S. Delhalle, J. J. Pireaux, R. Caudano, and J. J. Verbist, J. Chem. Phys. 60, 595 (1974).

[23]M. L. Knotek and P. J. Feibelman, Phys. Rev. Lett. 40, 964 (1978).

[24]M. L. Knotek, V. O. Jones, and V. Rehn, Phys. Rev. Lett. 43, 300 (1979).

[25]B. B. Pate, M. L. Knotek, G. Lubriel, J. Kelber, and W. E. Spicer (to be published).

[26]The estimate appearing in Ref. 8 for diamond D3 is corrected for the measured difference in valence band emission between D3 and D4 (0.2 eV) so that a similar estimate for D4 can be made.